binding sites for p53, we introduced a mutation at each of these predicted sites in the −43/+541 luc vector, and compared the levels of transcriptional activity. As shown in Fig. 4B, similar to the mutation at +180, mutating the +196 region also significantly reduced transcriptional activity. Although incomplete on its own, the p53-binding motif in the +196 region was 6 bp distal to the motif in the +180 region. The two motifs separated by a 6 bp spacer length is consistent with the criteria for a p53-binding domain described by Vogelstein *et al.* [21]. These findings suggest that the motifs in the +180 and +196 regions might be targets for p53 binding.

To examine whether endogenous p53 actually binds to these regions in CCA cells, we performed chromatin immunoprecipitation (ChIP) assays using PCR analysis of the p53 binding domains regulating *ANX4* and *p21* after immunoprecipitation with the p53-specific anti-

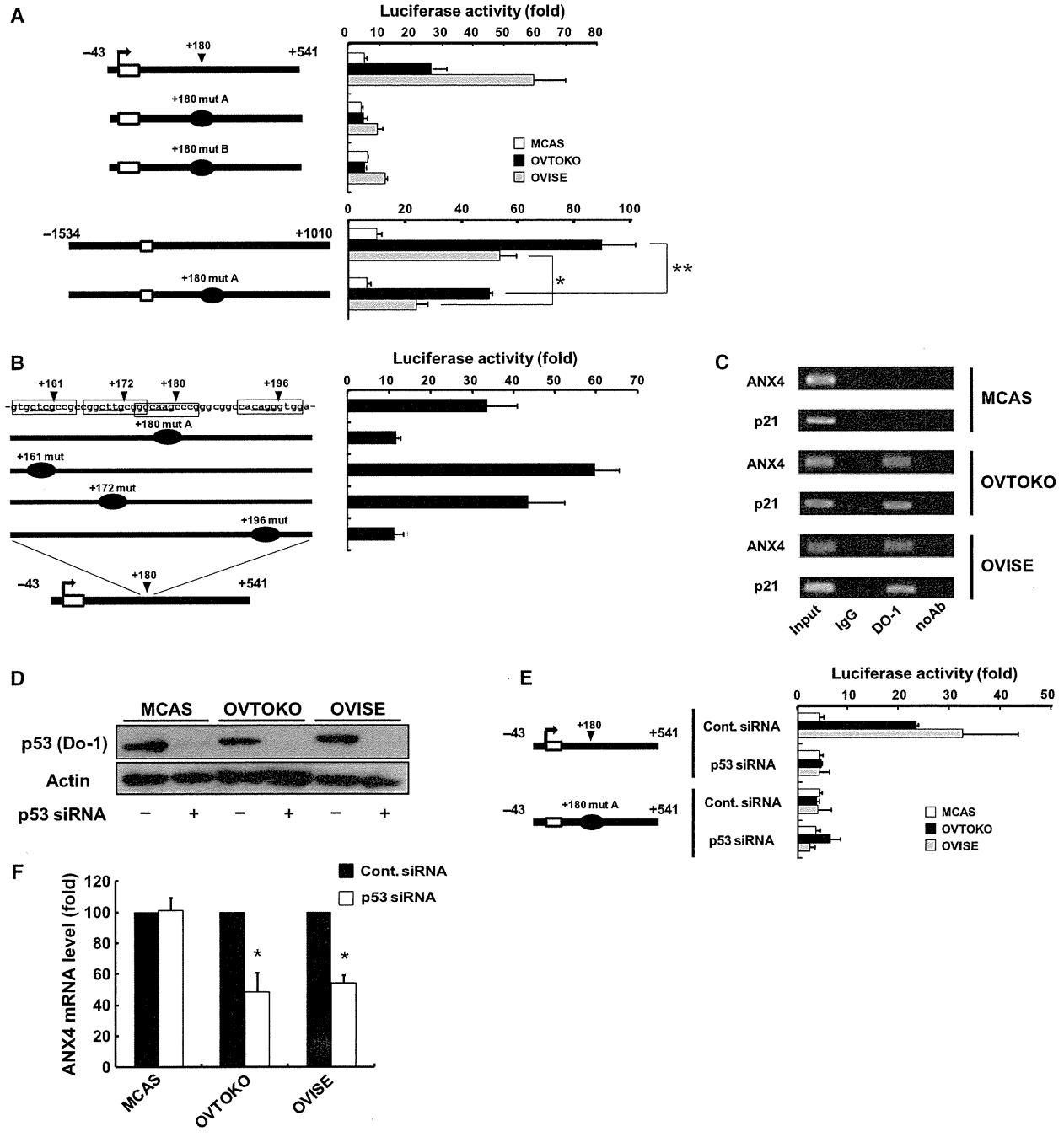

body DO-1 or normal IgG as a negative control. As shown in Fig. 4C, immunoprecipitation by the DO-1 antibody detected not only the *p21* promoter, but also the first intron of the *ANX4* gene in OVTOKO and OVISE cells but not in MCAS cells, indicating that endogenous p53 protein directly binds to the *ANX4* gene in CCA cells.

To verify the involvement of p53 in the CCA-specific expression of ANX4, we performed a gene-silencing experiment to suppress p53 protein expression. In cells transfected with a chemically modified small interfering RNA (siRNA) (Stealth™ siRNA) targeting p53 mRNA, the protein level of endogenous p53 markedly decreased (Fig. 4D). As shown in Fig. 4E, knockdown of p53 significantly reduced the transcriptional activity of the −43/+541 luc reporter in CCA cell lines but not in MCAS cells. By contrast, knockdown of p53 did not affect the activity of the reporter in any cell lines when the +180 region was mutated. These results indicate that p53 enhanced the transcriptional activity of *ANX4* via the +180 region. Similar data were obtained by knocking down p53 with another Stealth™ siRNA that targets a different site on the *p53* gene (data not shown). To confirm that the p53 protein actually regulates the expression of ANX4 mRNA, real-time RT-PCR analysis was conducted using the siRNA-transfected cells. As shown in Fig. 4F, introducing p53 siRNA reduced ANX4 mRNA in the CCA cell lines but did not affect ANX4 mRNA levels in the MCAS cells. These results indicate that *ANX4* is regulated by p53 in CCA cells.

Although the p53-directed siRNA completely diminished the CCA-specific transcriptional activity of the −43/+541 luc, it only reduced the ANX4 mRNA in CCA cells by approximately half. This discrepancy was also observed after mutations of the +180 region in the luciferase reporter vectors. In CCA cell lines, mutation of the +180 region completely diminished the transcriptional activity of −43/+541 luc, although the same mutation in −1534/+1010 luc, the reporter with the longest region, decreased transcriptional activity only by approximately half (Fig. 4A). Therefore, the transcriptional activation of *ANX4* in CCA is, at least in part, caused by p53, and other transcription factors with binding sites upstream of −43 or downstream of +541 might provide moderate additional transcriptional regulation.

ANX4 transcriptional activity correlates with the functional status of p53 in EOC cells

In almost all human cancers, p53 activity is lost as a result of mutation of the *p53* gene [22]. However, the above findings show that the *ANX4* gene is regulated by p53 in CCA cells, thereby suggesting that p53 is functional in CCA cells. To examine whether there is a correlation between the functional status of p53 and ANX4 transcriptional levels, we investigated *p53* gene mutations, as well as the expression levels of p53, ANX4 and typical p53 target genes. As shown in Fig. 5A, the p53 antibody DO-1 detected major bands near 53 kDa in EOC cell lines. Because the DO-1 antibody would also recognize p53β and p53γ, C-terminal truncated forms of the typical full-length p53 protein [23], the absence of bands at 46 kDa indicate that these proteins were not expressed in any of the EOC cell lines. Analysis of the *p53* cDNA sequences obtained from each cell line revealed no mutations in the CCA cell lines, whereas all non-CCA-type EOC cell lines had *p53* mutations (Table 1). Although the levels of p53 protein were lower in CCA cell lines, those of p53 target genes, p21 and murine double minute 2 (MDM2), as well as ANX4, were significantly higher in CCA cell lines than non-CCA-type EOC cell lines (Fig. 5A). In addition, in other cell lines carrying the wild-type *p53* gene, HEK293 or LNCaP cell lines, protein levels of ANX4, p21 and MDM2 were undetectable by western blotting (data not shown). Similar results were obtained by real time RT-PCR analyses; the mRNA levels of *p21* and *MDM2* were relatively lower in either HEK293, LNCaP or non-CCA-type EOC cell lines, which did not abundantly express ANX4 (Fig. 5B). These results suggest that there is a correlates between the functional status of p53 and ANX4 expression.

Wild-type p53 enhances the expression of the ANX4 gene

The results reported above suggest that the activation of wild-type p53 is one factor leading to ANX4 up-regulation in CCA. To examine whether wild-type p53 is actually involved in the transcriptional activation of *ANX4*, we transfected the −43/+541 luc and an expression plasmid containing wild-type p53 cDNA into MCAS, HEK293 and LNCaP cells (in which ANX4 levels are very low) and then conducted a luciferase assay. As shown in Fig. 6A, the overexpression of wild-type p53 resulted in a marked increase in *ANX4* transcriptional activity in each cell line. By contrast, transfection with the p53 mutants found in the non-CCA-type EOC cell lines, MCAS or OVCAR-3, did not alter luciferase activities in MCAS, HEK293 or LNCaP cells. As shown in Fig. 6B, ANX4 mRNA levels were substantially increased with the induction

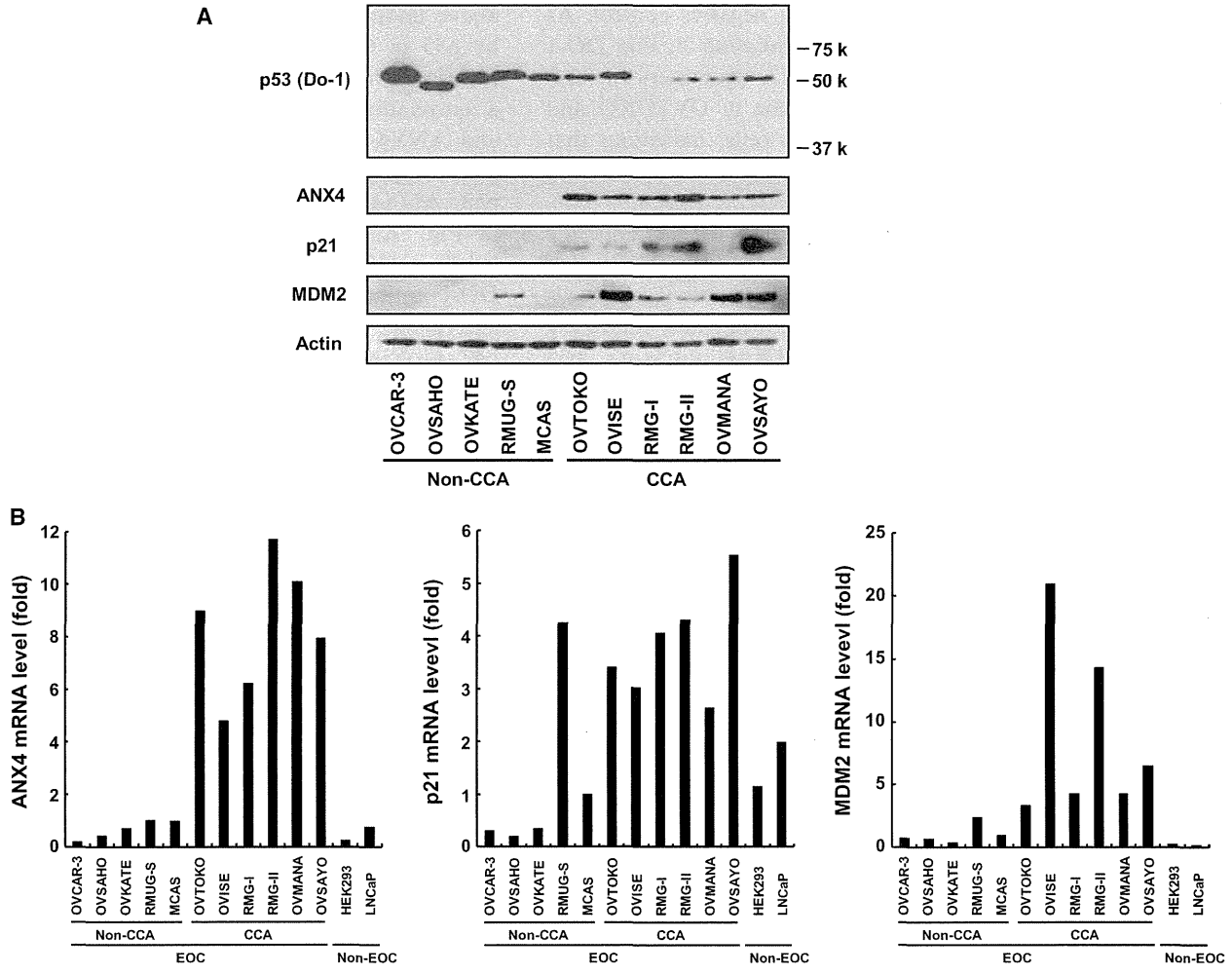

Fig. 5. ANX4 expression level correlates with p53 functional status. Protein and total RNA were extracted from various EOC cell lines, HEK293 and LNCaP cell lines. (A, B) Expression levels of protein and mRNA, and levels of p53, ANX4 and the known p53 targets, p21 and MDM2, were analyzed by western blotting (A) and real-time RT-PCR analyses (B), respectively. Actin protein levels were included in the western blotting analysis as a loading control. The relative mRNA levels were normalized to the level of 18S ribosomal RNA expression in each sample.

Table 1. p53 mutation lines used in the present study.

Cell line	Exon	Codon	Mutation	Amino acid change	EOC subtype
OVCAR-3	7	248	cgg → cag	R → Q	Serous
OVSAHO	10	342	cga → tga	R → Stop	Serous
OVKATE	8	282	cgg → tgg	R → W	Serous
RMUG-S	4, 10	72, 347	cgc → ccc, gcc → gtc	R → P, A → V	Mucinous
MCAS	4	114–125	Alternative sequence	LHSGTAKSVTCT → FTLWLP	Mucinous
OVTOKO	–	–	Not detected	–	Clear cell
OVISE	–	–	Not detected	–	Clear cell
RMG-I	–	–	Not detected	–	Clear cell
RMG-II	–	–	Not detected	–	Clear cell
OVMANA	–	–	Not detected	–	Clear cell
OVSAYO	–	–	Not detected	–	Clear cell
HEK293	–	–	Not detected	–	–
LNCaP	–	–	Not detected	–	–

of p21 mRNA in HEK293 cells transfected with the wild-type p53 expression vector. An increase in ANX4 mRNA was not observed in response to the overexpression of the p53 mutants. Moreover, when LNCaP cells, which endogenously express wild-type p53, were treated with the p53-activating reagent mitomycin C (MMC) or nutlin-3, p21 mRNA and protein levels were elevated along with increase in endogenous p53. Activation of endogenous p53 also increased mRNA and protein levels for ANX4 in LNCaP cells (Fig. 6C, D). These findings support the conclusion that wild-type p53 plays a role in the up-regulation of *ANX4*.

Discussion

The expression of ANX4 is specifically and characteristically enhanced in ovarian CCA cells. This suggests that the expression of *ANX4* is regulated by a molecular mechanism that is unique to these cells. However, the mechanisms for *ANX4* up-regulation in CCA cells have not been elucidated. In the present study, we identified tandem repeats corresponding to the motif for p53 binding in the first intron of the *ANX4* gene, and found (using reporter gene analysis) that this region is a key site for CCA-specific expression. Gene silencing of p53 by siRNA restricted ANX4 transcrip-

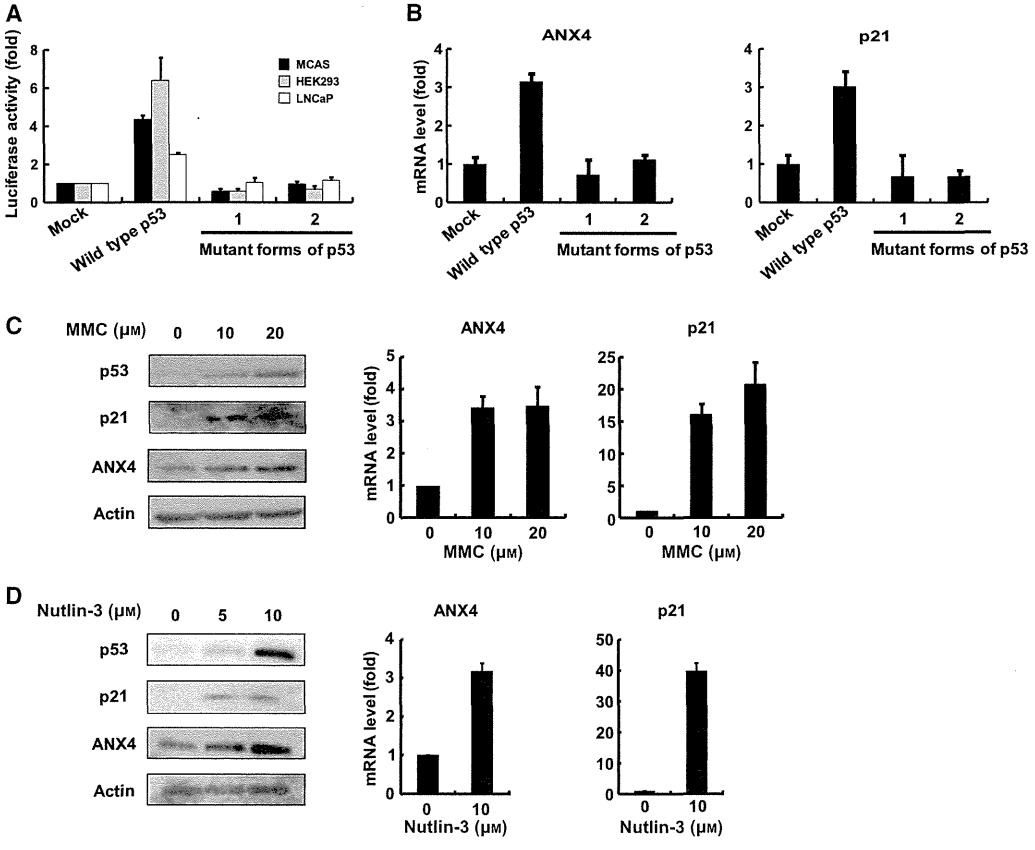

Fig. 6. Wild-type p53 induces *ANX4* gene expression. (A) The overexpression of wild-type p53 enhances the transcriptional activity of the *ANX4*-luciferase reporter. The −43/+541 luc was co-transfected into MCAS, HEK293 and LNCaP with pcDNA3 plasmids encoding the wild-type or mutant forms of p53. Mutant forms 1 and 2 were p53 cDNA cloned from OVCAR-3 and MCAS, respectively. After 48 h, luciferase activity was determined for each sample. The Renilla luciferase reporter vector was co-transfected as an internal control. (B) Overexpression of wild-type p53 activates the expression of ANX4. Wild-type or mutated p53 expression vectors were transfected into HEK293. After 48 h, total RNA was extracted and ANX4 mRNA levels were measured by real-time RT-PCR analyses. (C, D) ANX4 expression increased after p53 activation by MMC or nutlin-3 exposure. LNCaP cells were treated with MMC (C) or nutlin-3 (D). After treatment with MMC for 24 h or nutlin-3 for 12 h at the indicated concentrations, mRNA and protein levels of ANX4 and p21 were measured by western blotting and real-time RT-PCR analyses. The p53 protein levels were also assessed by western blotting to verify that MMC and nutlin-3 activated p53 effectively. The relative mRNA levels were normalized to the level of 18S ribosomal RNA expression in each sample. Actin protein levels were included in the western blotting analysis as a loading control. Bars represent the mean ± SE of three experiments.

tion in CCA cells but not in non-CCA-type EOC cells. No mutations of the *p53* gene were observed in any of the CCA-derived cell lines used in the present study, and p21 and MDM2 transcript levels were relatively higher compared to those in other cell lines in which ANX4 is not abundantly expressed. Moreover, the mRNA levels of ANX4 in other types of cell lines were significantly increased by the overexpression or activation of wild-type p53. Therefore, we conclude that wild-type p53 acts as a positive regulator of ANX4 expression in CCA cells.

The characteristic up-regulation of ANX4 in CCA led us to consider that the protein might be involved in the malignance of CCA by conferring drug resistance or accelerating cancer development. Unexpectedly, we found that the expression of the *ANX4* gene is directly regulated by the tumor suppressor protein p53 in CCA cells. In general, p53 is known to serve as a key player in responding to cellular stresses such as DNA damage, oncogenic activation and microtubule disruption [24,25]. When p53 is activated by such cellular stress, the protein exerts its effect mainly through the transcriptional activation of target genes, including p21, which arrests the cell cycle, and BAX, which induces apoptosis. Thus, p53 typically suppresses cancer development, preventing the division of damaged cells likely to contain mutations and exhibit abnormal cellular growth [26]. Indeed, the *p53* gene is mutated frequently in almost all human cancers [22]. However, among the EOC cell lines used in the present study, *p53* mutations were not observed in any of the CCA-type cell lines, although they were detected in all non-CCA cell lines, which express very low levels of ANX4 (Fig. 5B and Table 1). These findings are in good agreement with studies reporting that *p53* mutations are infrequent in ovarian CCA but occur in at least 50% of the other subtypes of EOC [6–9]. Furthermore, the overexpression of wild-type p53 resulted in an increase in the number of p21 and ANX4 transcripts, whereas overexpressing p53 mutants found in non-CCA cell lines had no effect on the transcription of either gene (Fig. 6). These results show that the p53 mutants in non-CCA cells were inert, compatible with previous findings that *p53* mutations generally result in a loss of wild-type protein activity, dominant-negative activity [27] or an increase in the half-life of the protein by preventing ubiquitination [28]. Therefore, the absence of p53 mutation contributes to the up-regulation of ANX4 in CCA cells. Furthermore, the functional status of p53 was more important. Despite having an intact *p53* gene, HEK293 and LNCaP cell lines expressed trace amounts of ANX4 (Fig. 5). Expression levels of p21 or MDM2 are higher in CCA cell lines than those of HEK293 and LNCaP cell lines, showing a correlation with the expression level of ANX4. Previous immunohistological studies also showed that p21 and MDM2 protein is higher in many ovarian CCA tissues compared to that found in the other EOC subtypes [29,30]. The data obtained in the present study together with those of these previous reports suggest that p53 functional status is critical in governing the ANX4 up-regulation in EOC cells.

Several previous studies have suggested a close relationship between wild-type p53 and *ANX4* expression. ANX4 expression is elevated in renal clear cell carcinoma [31], where *p53* gene mutations are rare [32], and p21 expression has been confirmed by immunohistochemical methods [33]. Moreover, comprehensive expression analysis of p53-induced genes using the p53 temperature-sensitive cell model revealed that ANX4 mRNA was induced after the activation of p53 [34]. ChIP-on-chip analysis using lymphoblastoid cells exposed to ionizing radiation identified 38 kinds of p53-binding genes, and the *ANX4* gene was among the identified genes [35]. These studies strongly support our finding that activated wild-type p53 directly regulates the expression of ANX4 in CCA cells.

In general, p53 has been shown to induce not only genes involved in tumor suppression, such as those that arrest the cell cycle, induce apoptosis and show anti-angiogenic activity, but also oncogenes such as MDM2, p53-inducible protein with RING-H2 domain (*PIRH2*) and constitutively photomorphogenic 1 (*COP1*) [36–38]. These oncogenes are cellular ubiquitin-protein ligases that bind to the p53 protein directly and regulate cellular p53 levels through ubiquitination. The proteasomal degradation of the p53 protein, regulated by a negative feedback mechanism, has been shown to contribute to tumor development. Whether ANX4 should be classified as an oncogene or as a tumor suppressor remains unknown because little is known about its functional role, although ANX4 is reported to be involved in chemoresistance [15,20], activation of chloride ion channels [19], exocytosis [18] and membrane permeability [17]. To clarify the functional and physiological role of the ANX4 protein in ovarian CCA, we are currently conducting proteomic analyses to identify its binding partners.

Because ovarian CCA shows a lower response to the standard paclitaxel–carboplatin combination chemotherapy, a patient with this disease has a worse prognosis than patients with other EOC subtypes, especially serous adenocarcinoma [2]. In CCA, *p53* mutation is infrequently observed [8,9]. Some studies have investigated whether the presence of *p53* mutations correlates with the response to platinum-based

chemotherapy in EOC patients. Lavarino *et al.* [39] and Ueno *et al.* [40] found that, overall, EOCs with wild-type p53 are less responsive to paclitaxel-carboplatin chemotherapy than EOCs with mutated p53 [39,40]. Moreover, when Ueno *et al.* [40] investigated individual EOC subtypes, they observed that this correlation apparently existed in EOC subtypes other than the serous type. Two other interesting studies have reported the suggested involvement of ANX4 in the chemoresistance of human cancer cell lines. Han *et al.* [20] found that the level of ANX4 protein expression was higher in a paclitaxel-resistant cell line derived from a lung cancer cell line than in the parent cell line, and that overexpression of ANX4 cDNA enhanced resistance to paclitaxel in HEK293T cells. Moreover, Kim *et al.* [15] also investigated whether ANX4 was associated with chemoresistance in EOC cell lines, and found that an ANX4-overexpressing cell line derived from the serous-type EOC cell line OVSAHO exhibited greater resistance to carboplatin compared to the parental cell line [15]. Taken together, the findings of these previous studies and our own reveal an association between p53 and ANX4 expression that suggests that tumor cells carrying wild-type p53, such as CCA, may exhibit chemoresistance conferred by p53-dependent ANX4 expression.

In conclusion, analysis of molecular mechanisms underlying CCA-specific ANX4 expression has revealed that the functional status of p53 is involved in the gene regulation in EOC cells. This may lead to a better understanding of the physiological significance of ANX4 up-regulation and the mechanisms underlying malignant progression and chemoresistance in CCA.

Experimental procedures

Cell cultures

Three ovarian cancer cell lines were used for most of the experiments in this study: OVTOKO and OVISE established from ovarian CCA [41], and MCAS, a cell line originating from ovarian mucinous cystadenocarcinoma cloned, as described previously [13]. In some experiments, eight more ovarian cancer cell lines were also used to verify our results. OVKATE, OVSAHO, OVMANA and OVSAYO were established from metastasis ovarian tumors by Yanagibashi *et al.* [42]. OVCAR-3 was obtained from the RIKEN (Tsukuba, Japan) cell bank, and RMUG-S, RMG-I and RMG-II were purchased from the Japanese Collection of Research Bioresources (Tokyo, Japan). RMUG-S, RMG-I and RMG-II were maintained in Ham's F-12 medium, and the other cell lines were cultured in RPMI medium. The human embryonic kidney cell line HEK293 and the prostate adenocarcinoma cell line LNCaP were grown in Ham's F-12 and RPMI 1690 mediums, respectively. All media were supplemented with 10% fetal bovine serum (JRH Biosciences, Inc., Lenexa, KS, USA). Cells were kept at 37 °C in a humidified atmosphere supplemented with 5% CO_2.

Western blotting

Protein was extracted from cells using 30 mM Tris-HCl buffer (pH 7.5) containing 7 M urea, 2 M thiourea, 4% Chaps and 1% dithithreitol. The protein extracts were separated by SDS/PAGE, transferred to poly(vinylidene difluoride) membranes, and blocked by incubation in the reagent Blocking One (Nacalai Tesque, Kyoto, Japan). The blots were then reacted with one of the primary antibodies: goat polyclonal anti-ANX4 (N-19), goat polyclonal anti-actin (I-19), rabbit polyclonal anti-p21 (C-19) and mouse monoclonal anti-MDM2 (SMP-14); all purchased from Santa Cruz Biotechnology (Santa Cruz, CA, USA). Mouse monoclonal anti-ANX4 (No. 50) and anti-p53 (DO-1) were purchased from Funakoshi (Tokyo, Japan) and Calbiochem (San Diego, CA, USA), respectively. Primary antibodies were detected using the ECL Plus Western Blotting Detection System (GE Healthcare, Milwaukee, WI, USA).

Real-time RT-PCR

Total RNA was isolated from the various cell lines using the RNeasy Plus Micro Kit (Qiagen, Hilden, Germany). cDNA was synthesized from the isolated RNA by reverse transcription with the oligo-dT primer and the 18S-rRNA specific primer as described in Zhu and Altmann [43] with one modification, namely, the use of the PrimeScript RT reagent (Takara Bio Inc., Shiga, Japan). Real-time PCR was performed using the Mx3000P Real-Time QPCR System (Agilent Technologies, Santa Clara, CA, USA) with SYBR Premix Ex Taq™ II Perfect Real Time (Takara Bio Inc.). The primer pairs indicated in Table S1 were used for the reactions at a concentration of 10 μM. The PCR products were detected by monitoring the increase in reporter dye fluorescence. mRNA levels were normalized to 18S ribosomal RNA levels.

5′-RACE analysis

Total RNAs isolated from OVTOKO, OVISE and MCAS were reverse-transcribed using the PowerScript reverse transcriptase (Clontech Laboratories, Palo Alto, CA, USA) with the ANX4-RT primer, which is complementary to the nucleotide sequence of the human ANX4 mRNA (GenBank accession number: BC001153). dCTP tails were added to the cDNAs using terminal deoxytransferase (Invitrogen, Carlsbad, CA, USA), and then PCR amplification was per-

formed with the oligo-dI-dG primer and the ANX4-R01 primer (Table S2). The RACE end determined by sequencing analysis was regarded as the transcription start site of *ANX4* and denoted as +1.

Plasmids

For production of luciferase reporter constructs, the flanking region of the transcription start site of *ANX4*, from −1534 to +1010, was amplified from human genomic DNA (Novagen, Darmstadt, Germany) by PCR using KOD-plus DNA polymerase (Toyobo Life Science, Osaka, Japan), and then cloned into the *SmaI*/*BglII* site of pGL3-basic vector (Promega, Madison, WI, USA). The 5′- or 3′-deletion constructs were produced by reacting the amplified PCR products using the primers shown in Table S2 with restriction enzymes. Deletions and mutations in the +180 region were performed by ligating two PCR fragments amplified with a mutation primer, as described previously [44]. To construct the wild-type and mutated p53 expression vectors, full-length p53 cDNAs were isolated from OVISE, OVCAR-3 and MCAS by PCR amplification and then cloned into the *Hind*III/*Eco*RV site of the pcDNA3.1 plasmid (Invitrogen). All constructs were sequenced to verify the orientation and fidelity of the insert.

Luciferase reporter assay

EOC cell lines were seeded on 24-well plates at a density of 2.0×10^5, 3.0×10^5 and 2.5×10^5 cells per well for MCAS, OVTOKO and the other cell lines, respectively. After 24 h, cells were transfected with a pGL3 reporter vector and a pSV-β-galactosidase control vector as an internal control (Promega) using FuGENE HD (Roche, Indianapolis, IN, USA) in accordance with the manufacturer's instructions. For experiments in which p53 was overexpressed, the pRL-TK vector (Promega) was used as an internal control. Then, 42 h after transfection, luciferase activity in cell lysates was measured and normalized to either β-galactosidase activity or Renilla luciferase activity.

ChIP

ChIP assays were performed using the ChIP-IT kit (Active Motif, Carlasbad, CA, USA) in accordance with the manufacturer's instructions. In brief, OVISE, OVTOKO and MCAS cells at 70–80% confluence in 15 cm plates were fixed for 15 min at room temperature with 1% formaldehyde. To shear genomic DNA, the nuclei were subjected to enzymatic digestion with 5 units of enzymatic shearing mixture solution (Active Motif) for 15 min at 37 °C. Sheared chromatin was immunoprecipitated with 4 μg of anti-p53 (DO-1; Calbiochem) or control IgG (Active Motif). Cross-linking was reversed and purified DNA was subjected to PCR. The PCR products were analyzed by electrophoresis on a 2% agarose gel stained with ethidium bromide. Primers employed were designed to detect the predicted p53 binding sites on *ANX4* and *p21* genes. The primer sequences are indicated in Table S3.

Gene silencing of p53

Stealth™ siRNAs (Invitrogen) were used to silence the *p53* gene. Two kinds of Stealth™ siRNAs were tested for their RNA interference (RNAi) activity against the *p53* gene, and the one resulting in a higher level of knockdown was selected for further use. The targeted sequence of the selected siRNA was 5′-UGGAAGACUCCAGUGGUAAUCUACU-3′, corresponding to nucleotides 890–914 of the p53 mRNA (GenBank accession number: BC003596). Control experiments used the Stealth™ RNAi negative control MED (Invitrogen). EOC cells were transfected with the Stealth™ siRNAs using Lipofectamine RNAi MAX (Invitrogen) in accordance with the manufacturer's instructions. For the luciferase assay, siRNA-transfected cells were incubated for 24 h in one well of a 24-well plate, and then transfected with reporter vectors. For western blotting or real-time RT-PCR analyses, all cell lines were transfected with siRNA and grown for 72 h.

p53 mutation analysis

The p53 cDNAs from various cell lines were amplified by PCR using the KOD-plus DNA polymerase (Toyobo Life Science) and *p53*-specific primers (sense 5′-CACGACGGT GACACGCTTCC-3′ and antisense 5′-CCTGGGTGCTT CTGACGCAC-3′) corresponding to nucleotides 64–83 and 1404–1423 of the p53 mRNA, respectively (GenBank accession number: BC003596). The PCR products were purified using the Wizard SV Gel and the PCR Clean-Up System (Promega) and then subjected to sequence analyses.

p53 activation by drug treatment

LNCaP cells were grown to 60–70% confluency in six-well plates, and then treated with different concentrations of MMC (Calbiochem) for 24 h, or nutlin-3 (Cayman Chemical, Ann Arbor, MI, USA) for 12 h. After treatment, cells were subjected to real-time RT-PCR and western blotting.

Acknowledgements

This work was supported in part by a Grant-in-Aid for young Scientists (B) 18790226 and 20790262 from The Ministry of Education, Culture, Sports, Science and Technology, Japan. We thank Dr Youhei Miyagi (Kanagawa Cancer Center, Kanagawa, Japan) and Dr Masato Katsuyama (Kyoto Prefectural University of Medicine, Kyoto, Japan) for insightful discussions.

References

1 Bray F, Loos AH, Tognazzo S & La Vecchia C (2005) Ovarian cancer in Europe: cross-sectional trends in incidence and mortality in 28 countries, 1953-2000. *Int J Cancer* **113**, 977–990.

2 Sugiyama T, Kamura T, Kigawa J, Terakawa N, Kikuchi Y, Kita T, Suzuki M, Sato I & Taguchi K (2000) Clinical characteristics of clear cell carcinoma of the ovary: a distinct histologic type with poor prognosis and resistance to platinum-based chemotherapy. *Cancer* **88**, 2584–2589.

3 Itamochi H, Kigawa J, Akeshima R, Sato S, Kamazawa S, Takahashi M, Kanamori Y, Suzuki M, Ohwada M & Terakawa N (2002) Mechanisms of cisplatin resistance in clear cell carcinoma of the ovary. *Oncology* **62**, 349–353.

4 Itamochi H, Kigawa J, Sugiyama T, Kikuchi Y, Suzuki M & Terakawa N (2002) Low proliferation activity may be associated with chemoresistance in clear cell carcinoma of the ovary. *Obstet Gynecol* **100**, 281–287.

5 Itamochi H, Kigawa J & Terakawa N (2008) Mechanisms of chemoresistance and poor prognosis in ovarian clear cell carcinoma. *Cancer Sci* **99**, 653–658.

6 Marks JR, Davidoff AM, Kerns BJ, Humphrey PA, Pence JC, Dodge RK, Clarke-Pearson DL, Iglehart JD, Bast RC Jr & Berchuck A (1991) Overexpression and mutation of p53 in epithelial ovarian cancer. *Cancer Res* **51**, 2979–2984.

7 Kohler MF, Marks JR, Wiseman RW, Jacobs IJ, Davidoff AM, Clarke-Pearson DL, Soper JT, Bast RC Jr & Berchuck A (1993) Spectrum of mutation and frequency of allelic deletion of the p53 gene in ovarian cancer. *J Natl Cancer Inst* **85**, 1513–1519.

8 Ho ES, Lai CR, Hsieh YT, Chen JT, Lin AJ, Hung MH & Liu FS (2001) p53 mutation is infrequent in clear cell carcinoma of the ovary. *Gynecol Oncol* **80**, 189–193.

9 Okuda T, Otsuka J, Sekizawa A, Saito H, Makino R, Kushima M, Farina A, Kuwano Y & Okai T (2003) p53 mutations and overexpression affect prognosis of ovarian endometrioid cancer but not clear cell cancer. *Gynecol Oncol* **88**, 318–325.

10 Saegusa M, Machida BD & Okayasu I (2001) Possible associations among expression of p14(ARF), p16(INK4a), p21(WAF1/CIP1), p27(KIP1), and p53 accumulation and the balance of apoptosis and cell proliferation in ovarian carcinomas. *Cancer* **92**, 1177–1189.

11 Schaner ME, Ross DT, Ciaravino G, Sorlie T, Troyanskaya O, Diehn M, Wang YC, Duran GE, Sikic TL, Caldeira S *et al.* (2003) Gene expression patterns in ovarian carcinomas. *Mol Biol Cell* **14**, 4376–4386.

12 Schwartz DR, Kardia SL, Shedden KA, Kuick R, Michailidis G, Taylor JM, Misek DE, Wu R, Zhai Y, Darrah DM *et al.* (2002) Gene expression in ovarian cancer reflects both morphology and biological behavior, distinguishing clear cell from other poor-prognosis ovarian carcinomas. *Cancer Res* **62**, 4722–4729.

13 Morita A, Miyagi E, Yasumitsu H, Kawasaki H, Hirano H & Hirahara F (2006) Proteomic search for potential diagnostic markers and therapeutic targets for ovarian clear cell adenocarcinoma. *Proteomics* **6**, 5880–5890.

14 Zhu Y, Wu R, Sangha N, Yoo C, Cho KR, Shedden KA, Katabuchi H & Lubman DM (2006) Classifications of ovarian cancer tissues by proteomic patterns. *Proteomics* **6**, 5846–5856.

15 Kim A, Enomoto T, Serada S, Ueda Y, Takahashi T, Ripley B, Miyatake T, Fujita M, Lee CM, Morimoto K *et al.* (2009) Enhanced expression of annexin A4 in clear cell carcinoma of the ovary and its association with chemoresistance to carboplatin. *Int J Cancer* **125**, 2316–2322.

16 Moss SE & Morgan RO (2004) The annexins. *Genome Biol* **5**, 219.

17 Hill WG, Kaetzel MA, Kishore BK, Dedman JR & Zeidel ML (2003) Annexin A4 reduces water and proton permeability of model membranes but does not alter aquaporin 2-mediated water transport in isolated endosomes. *J Gen Physiol* **121**, 413–425.

18 Sohma H, Creutz CE, Gasa S, Ohkawa H, Akino T & Kuroki Y (2001) Differential lipid specificities of the repeated domains of annexin IV. *Biochim Biophys Acta* **1546**, 205–215.

19 Xie W, Kaetzel MA, Bruzik KS, Dedman JR, Shears SB & Nelson DJ (1996) Inositol 3,4,5,6-tetrakisphosphate inhibits the calmodulin-dependent protein kinase II-activated chloride conductance in T84 colonic epithelial cells. *J Biol Chem* **271**, 14092–14097.

20 Han EK, Tahir SK, Cherian SP, Collins N & Ng SC (2000) Modulation of paclitaxel resistance by annexin IV in human cancer cell lines. *Br J Cancer* **83**, 83–88.

21 el-Deiry WS, Kern SE, Pietenpol JA, Kinzler KW & Vogelstein B (1992) Definition of a consensus binding site for p53. *Nat Genet* **1**, 45–49.

22 Levine AJ, Momand J & Finlay CA (1991) The p53 tumour suppressor gene. *Nature* **351**, 453–456.

23 Bourdon JC, Fernandes K, Murray-Zmijewski F, Liu G, Diot A, Xirodimas DP, Saville MK & Lane DP (2005) p53 isoforms can regulate p53 transcriptional activity. *Genes Dev* **19**, 2122–2137.

24 Meek DW (1998) Multisite phosphorylation and the integration of stress signals at p53. *Cell Signal* **10**, 159–166.

25 Lane DP (1992) Cancer. p53, guardian of the genome. *Nature* **358**, 15–16.

26 Ryan KM, Phillips AC & Vousden KH (2001) Regulation and function of the p53 tumor suppressor protein. *Curr Opin Cell Biol* **13**, 332–337.

27 Levesque MA, Katsaros D, Yu H, Zola P, Sismondi P, Giardina G & Diamandis EP (1995) Mutant p53 protein overexpression is associated with poor outcome in patients with well or moderately differentiated ovarian carcinoma. *Cancer* **75**, 1327–1338.
28 Eltabbakh GH, Belinson JL, Kennedy AW, Biscotti CV, Casey G, Tubbs RR & Blumenson LE (1997) p53 overexpression is not an independent prognostic factor for patients with primary ovarian epithelial cancer. *Cancer* **80**, 892–898.
29 Shimizu M, Nikaido T, Toki T, Shiozawa T & Fujii S (1999) Clear cell carcinoma has an expression pattern of cell cycle regulatory molecules that is unique among ovarian adenocarcinomas. *Cancer* **85**, 669–677.
30 Skomedal H, Kristensen GB, Abeler VM, Borresen-Dale AL, Trope C & Holm R (1997) TP53 protein accumulation and gene mutation in relation to overexpression of MDM2 protein in ovarian borderline tumours and stage I carcinomas. *J Pathol* **181**, 158–165.
31 Zimmermann U, Balabanov S, Giebel J, Teller S, Junker H, Schmoll D, Protzel C, Scharf C, Kleist B & Walther R (2004) Increased expression and altered location of annexin IV in renal clear cell carcinoma: a possible role in tumour dissemination. *Cancer Lett* **209**, 111–118.
32 Hsueh C, Wang H, Gonzalez-Crussi F, Lin JN, Hung IJ, Yang CP & Jiang TH (2002) Infrequent p53 gene mutations and lack of p53 protein expression in clear cell sarcoma of the kidney: immunohistochemical study and mutation analysis of p53 in renal tumors of unfavorable prognosis. *Mod Pathol* **15**, 606–610.
33 Weiss RH, Borowsky AD, Seligson D, Lin PY, Dillard-Telm L, Belldegrun AS, Figlin RA & Pantuck AD (2007) p21 is a prognostic marker for renal cell carcinoma: implications for novel therapeutic approaches. *J Urol* **177**, 63–68.
34 Robinson M, Jiang P, Cui J, Li J, Wang Y, Swaroop M, Madore S, Lawrence TS & Sun Y (2003) Global genechip profiling to identify genes responsive to p53-induced growth arrest and apoptosis in human lung carcinoma cells. *Cancer Biol Ther* **2**, 406–415.
35 Jen KY & Cheung VG (2005) Identification of novel p53 target genes in ionizing radiation response. *Cancer Res* **65**, 7666–7673.
36 Li M, Brooks CL, Wu-Baer F, Chen D, Baer R & Gu W (2003) Mono- versus polyubiquitination: differential control of p53 fate by Mdm2. *Science* **302**, 1972–1975.
37 Leng RP, Lin Y, Ma W, Wu H, Lemmers B, Chung S, Parant JM, Lozano G, Hakem R & Benchimol S (2003) Pirh2, a p53-induced ubiquitin-protein ligase, promotes p53 degradation. *Cell* **112**, 779–791.
38 Dornan D, Wertz I, Shimizu H, Arnott D, Frantz GD, Dowd P, O'Rourke K, Koeppen H & Dixit VM (2004) The ubiquitin ligase COP1 is a critical negative regulator of p53. *Nature* **429**, 86–92.
39 Lavarino C, Pilotti S, Oggionni M, Gatti L, Perego P, Bresciani G, Pierotti MA, Scambia G, Ferrandina G, Fagotti A *et al.* (2000) p53 gene status and response to platinum/paclitaxel-based chemotherapy in advanced ovarian carcinoma. *J Clin Oncol* **18**, 3936–3945.
40 Ueno Y, Enomoto T, Otsuki Y, Sugita N, Nakashima R, Yoshino K, Kuragaki C, Ueda Y, Aki T, Ikegami H *et al.* (2006) Prognostic significance of p53 mutation in suboptimally resected advanced ovarian carcinoma treated with the combination chemotherapy of paclitaxel and carboplatin. *Cancer Lett* **241**, 289–300.
41 Gorai I, Nakazawa T, Miyagi E, Hirahara F, Nagashima Y & Minaguchi H (1995) Establishment and characterization of two human ovarian clear cell adenocarcinoma lines from metastatic lesions with different properties. *Gynecol Oncol* **57**, 33–46.
42 Yanagibashi T, Gorai I, Nakazawa T, Miyagi E, Hirahara F, Kitamura H & Minaguchi H (1997) Complexity of expression of the intermediate filaments of six new human ovarian carcinoma cell lines: new expression of cytokeratin 20. *Br J Cancer* **76**, 829–835.
43 Zhu LJ & Altmann SW (2005) mRNA and 18S-RNA coapplication-reverse transcription for quantitative gene expression analysis. *Anal Biochem* **345**, 102–109.
44 Kato Y, Arakawa N, Masuishi Y, Kawasaki H & Hirano H (2009) Mutagenesis of longer inserts by the ligation of two PCR fragments amplified with a mutation primer. *J Biosci Bioeng* **107**, 95–97.

Supporting information

The following supplementary material is available:
Fig. S1. The +180 region is essential for CCA-specific transcriptional activity of *ANX4*.
Table S1. Nucleotide sequences of the primers used in real-time RT-PCR.
Table S2. Nucleotide sequences of the primers used for 5′-RACE and plasmid construction.
Table S3. Nucleotide sequences of the primers used in the ChIP assay.

This supplementary material can be found in the online version of this article.

Please note: As a service to our authors and readers, this journal provides supporting information supplied by the authors. Such materials are peer-reviewed and may be re-organized for online delivery, but are not copy-edited or typeset. Technical support issues arising from supporting information (other than missing files) should be addressed to the authors.

Cancer Biomarkers 10 (2011/2012) 175–183
DOI 10.3233/CBM-2012-0243
IOS Press

Use of quantitative shotgun proteomics to identify fibronectin 1 as a potential plasma biomarker for clear cell carcinoma of the kidney

Akira Yokomizo[a,*,1], Michiko Takakura[b,1], Yae Kanai[c], Tomohiro Sakuma[d], Junichi Matsubara[b], Kazufumi Honda[b], Seiji Naito[a], Tesshi Yamada[b] and Masaya Ono[b]
[a]*Department of Urology, Graduate School Medical Sciences, Kyushu University, Fukuoka, Japan*
[b]*Division of Chemotherapy and Clinical Research, National Cancer Center Research Institute, Tokyo, Japan*
[c]*Division of Molecular Pathology, National Cancer Center Research Institute, Tokyo, Japan*
[d]*BioBusiness Group, Mitsui Knowledge Industry, Tokyo, Japan*

Abstract. *Background*: Early detection would be one of the most effective means to improve the outcome of renal cell carcinoma (RCC). We searched for a new plasma marker for RCC using a label-free quantitative shotgun proteomics method.
Methods: Plasma proteins were digested by trypsin, and the resulting peptides were analyzed by 2-Dimensional Image Converted Analysis of Liquid chromatography mass spectrometry (2DICAL). An identified biomarker candidate was subjected to validation using the Amplified Luminescent Proximity Homogeneous Assay (AlphaLISA).
Results: Among a total of 23,407 independent MS peaks, we found that the mean intensity of 59 peaks significantly differed between 20 clear cell RCC patients and 20 healthy controls. MS/MS spectra from 16 of the 59 peaks matched the amino acid sequences of the fibronectin 1 (*FN1*) gene product. The increased plasma level of FN1 in RCC patients was validated in a cohort of in 77 patients and 130 healthy controls ($p < 0.0001$).
Conclusions: The FN1 is considered to be a promising biomarker candidate for clear cell RCC. Furthermore, AlphaLISA is an alternate to the conventional enzyme-linked immunosorbent assay and should prove useful for the rapid validation of biomarker candidates.

Keywords: Renal cell carcinoma, tumor marker, proteomics, fibronectin

1. Introduction

The incidence of renal cell carcinoma (RCC) has been increasing since 1980s in western countries as well as Japan and is now the third most common malignancy of the urinary tract following prostate and bladder cancers [1]. Although early detection and treatment are considered to be the most effective methods to improve the outcome of patients with any cancer, RCC patients often do not manifest clinical symptoms and receive medical attention until their tumors progress to advanced stages [2–4]. Recently, ultrasound and CT scan can detect smaller renal tumors. However, we do need an effective plasma biomarker for differentiating the malignant from the benign when a patient was found with a small renal mass, which cannot be easily judged from ultrasound or CT scan [5]. Therefore, it is necessary to identify the tumor marker better than neither ultrasound test nor CT scan in diagnosing small renal mass. If a sensitive but non-invasive blood assay that can detect early-stage RCC were available, it would greatly improve the curative rate of RCC.

Shotgun proteomics is an established technique in which whole proteins are enzymatically digested into a large array of small peptide fragments followed

*Corresponding author: Akira Yokomizo, Department of Urology, Graduate School of Medical Sciences, Kyushu University, 3-1-1 Maidashi, Higashi-ku, Fukuoka 812-8252, Japan. Tel.: +81 92 642 5603; Fax: +81 92 642 5618; E-mail: yokoa@uro.med.kyushu-u.ac.jp.
[1]These two authors contributed equally to this work.

by direct analysis by liquid chromatography and mass spectrometry (LC-MS). We previously developed software named 2DICAL that can provide a quantitative dimension to shotgun proteomics [6]. 2DICAL can accurately align different LC-MS data and compare the protein content of a theoretically unlimited number of samples without isotope labeling [7]. 2DICAL is highly advantageous methods in clinical studies that require the comparison of a statistically sufficient number of patient samples [8]. Using 2DICAL, we were able to identify diagnostic biomarkers for endometrial and pancreatic cancers [7,8] and predictive biomarkers for hematologic toxicities and therapeutic efficacy of gemcitabine treatment to patients with advanced pancreatic cancer [9].

In this study we compared the plasma proteome between RCC patients and healthy controls using 2DICAL with the aim to identify a new diagnostic biomarker that can be used for a blood test. RCC consists of clear cell (75%), papillary (10%), chromophobe (5%) and other subtypes [10], and we first focused on clear cell carcinoma, the most common subtype of RCC. We discovered a significant increase of circulating plasma FN1 in patients with RCC and confirmed its significance in a larger patient cohort using a newly established measurement system.

2. Materials and methods

2.1. Plasma samples

Plasma samples were prospectively collected from RCC patients, prostate cancer patients and healthy volunteers at the Department of Urology, Kyushu University Hospital (Fukuoka, Japan) between October 2000 and January 2008. To exclude sampling bias, all the patients' whole blood (7 ml) was collected in the same tube (EDTA-2Na tube, Venoject II, Terumo, Japan) before the surgery or first treatment. These blood samples were stored in 4°C for 1 hour and plasma was separated after centrifugation, aliquoted into 1 ml samples in 1.5 ml eppendorf tubes, and stored at −80°C. The control samples were collected and stored under the same condition. All the samples had the only one cycle of freeze-and-thaw. As we excluded the non-clear cell subtype and benign kidney tumors, the plasma from 77 histopathologically proven clear cell cancer patients were used for the analysis. Control plasma samples were randomly selected from 20 patients with prostate cancer and 130 healthy individuals after adjusting the age and gender. The clinical stage of each patient was classified according to the 7th edition UICC TNM classification [11]. Twenty RCC patients (excluding those in stage IV) were selected for analysis using 2DICAL in an effort to detect early stage biomarkers (Table 1).

2.2. Ethics

All individuals provided written informed consent authorizing the collection and use of their samples for research purposes. The protocol was reviewed and approved by the institutional ethics committee boards of the National Cancer Center Research Institute (Tokyo, Japan) and the Kyushu University (Fukuoka, Japan).

2.3. LC-MS

The 20 most abundant plasma proteins including albumin and immunoglobulin were removed using ProtPrep 20 Plasma Immunodepletion Kit (Sigma-Aldrich, St. Louis, MO) following the manufacturer's instructions. The depleted plasma samples were then digested with trypsin (Promega, Madison, WI) overnight at 37°C. The resulting peptides were randomized and measured in triplicate by LC-MS. LC separation in a linear gradient of 0 to 80% acetonitrile in 0.1% formic acid at a speed of 200 nL/minute for 60 minutes was conducted using a splitless nano-flow HPLC system (Hitachi High-technologies, Tokyo, Japan). MS data were acquired every second for 60 minutes by an electrospray ionization mass spectrometer (Q-TOF Ultima; Waters, Milford, MC) directly linked to an LC in the range of 250–1600 m/z. MS peaks were detected, normalized, and quantified using the in-house 2DICAL software package as described previously [7]. A serial ID number was applied to each of the MS peaks detected (ID 1 to 23,407) [9]. The stability of LC-MS was monitored by calculating the correlation coefficient (CC) and coefficient of variance (CV) values among triplicate measurements.

2.4. Protein identification by tandem mass spectrometry (MS/MS)

Peak lists were generated using the Mass Navigator software package (version 1.2) (Mitsui Knowledge Industry, Tokyo, Japan) and searched against the SwissProt database (SwissProt_57.6.fast) using the Mascot software package (version 2.2.06) (Matrix Science, London, UK). The search parameters used were as follows: A database of human proteins was selected.

Table 1
Clinicopathological characteristics of individuals examined in this study

		Cases anlyzed by AlphaLISA (n = 227)			Cases analyzed by 2DICAL (n = 60)	
		RCC (n = 77)	PCa (n = 20)	Healthy (n = 130)	RCC (n = 20)	Healthy (n = 20)
Age	(mean ± SD)	61.2 ± 11.0	64.8 ± 6.9	65.4 ± 10.5	63.8 ± 8.5	66.0 ± 7.9
Gender						
	Male	57	20	113	20	20
	Female	20		17	0	0
Clinical stage*						
	I	56	9		17	
	II	3	11		2	
	III	3			1	
	IV	9			0	
	Unknown	6				
Tumor side						
	Right	38			11	
	Left	39			9	
Histologic type						
	Clear cell	77			20	
	Chromophobe	0			0	
	Papillary	0			0	
	Unclassified	0			0	

*according to TNM Classification of Malignantu Tumors (International Union Against Cancer), 7th Edition
RCC, renal cell carcinome; PCa, prostate cancer; AlphaLISA, amplified luminescence proximity homogeneous assay; 2DICAL, two-dimensional image convert

Trypsin was designated as the enzyme, and up to one missed cleavage was allowed. Mass tolerances for precursor and fragment ions were ± 0.2 Da and ± 0.8 Da, respectively. The score threshold was set to the value over 20 for peptide search. If a peptide matched to multiple proteins, the protein name with the highest Mascot score was selected.

2.5. Western blot analysis

Plasma samples were fractionated with SDS-PAGE and electroblotted onto a polyvinylidene difluoride membrane (Millipore, Billerica, MA), as described previously [9,12]. Primary antibodies used were mouse monoclonal anti-FN1 antibody (R&D Systems, Minneapolis, MN) and mouse monoclonal antibody against human complement C3b-α (PROGEN, Heidelberg, Germany) [8]. The membrane was then incubated with the primary antibody and subsequently with the relevant horseradish peroxidase-conjugated anti-mouse IgG as described previously. Blots were developed using an enhanced chemiluminescence (ECL plus) detection system (GE Healthcare, Buckinghamshire, UK).

2.6. AlphaLISA

An assay for measuring soluble FN1 was constructed using the AlphaLISA system (PerkinElmer, MA) which is a bead-bead nonradioactive technology. In brief, when a biological interaction brings the beads into close proximity, a cascade of chemical reactions is induced resulting in a greatly amplified signal, then a photosensitizer present in the beads converts ambient oxygen to a more excited singlet state upon laser excitation. Biotinylated rabbit polyclonal anti-FN1 antibody and mouse polyclonal anti-FN1 antibody were purchased from Abcam (Cambridge, UK). The AlphaLISA procedure was carried out according to the protocol provided by the manufacturer.

2.7. Statistical methods

The Mann-Whitney U-test was employed for statistical analysis of the correlation between RCC patients and controls as well as the plasma values of FN1 and clinicopathological parameters. Welch's t-test was employed for 2DICAL analysis. Kaplan–Meier analysis was used to examine the correlation of the plasma value of FN1, cancer-specific survival and overall survival. The area under the curve (AUC) of the receiver operating characteristic (ROC) was calculated to evaluate its diagnostic significance.

3. Results

3.1. Identification of plasma proteins significantly increased in RCC patients

Plasma proteins of 20 patients with RCC and 20 healthy individuals were digested by trypsin, and

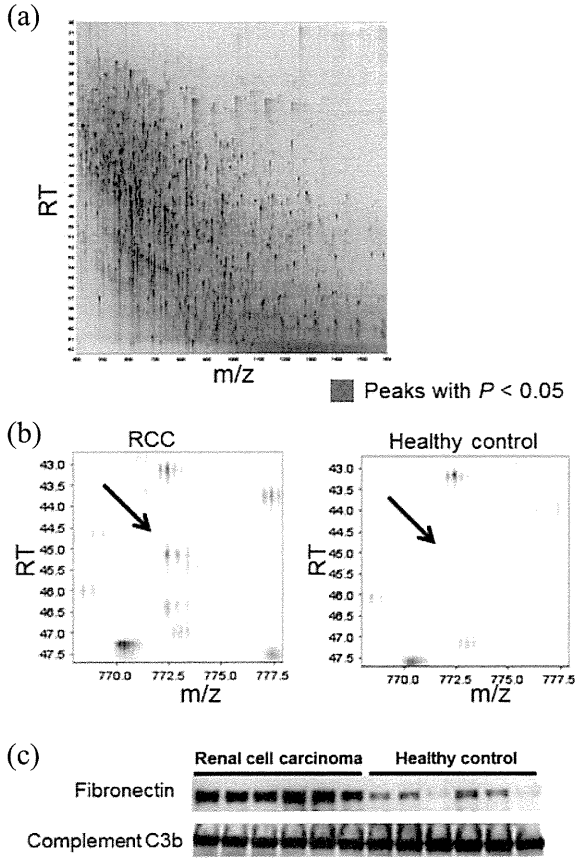

Fig. 1. (a) Two-dimensional display of all the MS peaks in 2DICAL. The 59 MS peaks whose mean intensity significantly differed in renal cell carcinoma patients from healthy controls ($p < 0.05$, Welch's t-test) are highlighted in red. (b) Two representative MS peaks with the smallest p-value. RT; retention time. (c) Detection of plasma FN1 and complement C3b-α (loading control) by immunoblotting.

the resulting peptides were subjected to LC-MS. A total of 23,407 MS peaks per sample were detected in the range of 250–1,600 m/z and 25–65 minutes across the 40 plasma samples, and their relative mass intensity was calculated using 2DICAL. The mean CC and CV values of the 23,407 MS peaks were over 0.95 and under 0.15, respectively, confirming the high reproducibility of LC-MS. Among the 23,407 MS peaks we found that the mean intensity of 59 peaks (in triplicate) significantly differed between 20 RCC patients and 20 healthy controls ($p < 0.05$, Welch's t-test). Thirty six peaks were increased and 23 peaks were decreased in RCC patients and the statistical significance was confirmed by calculating the false discovery rate (FDR) values [13] (data not shown). Figure 1a shows a representative 2-dimensional view in which all the ~23,000 MS peaks were displayed with the m/z along the X axis and the RT of LC along the Y axis and the 59 MS peaks are highlighted in red. Figure 1b shows a representative MS peak that increased in the plasma of RCC patients.

3.2. *Protein identification by MS/MS*

Fifty seven MS/MS spectra acquired from the 59 MS peaks matched to 21 peptide sequences deposited in the human protein database (Table 2). Remarkably, 16 of the 21 peptides were found to be derived from the amino acid sequence of *FN1* gene product (Supportive information Figs S1 and S2). The identification and differential expression of FN1 protein were confirmed by immunoblotting (Fig. 1c).

3.3. *Verification by AlphaLISA*

To validate the increased level of plasma FN1, we constructed a new assay that can quantify the amount of FN1. The AlphaLISA showed high reproducibility with a median CV value of 0.08 among triplicates and linearity in the range of 50–800 μg/ml.

The plasma concentration of FN1 was measured in 77 RCC patients, 20 prostate cancer (PCa) patients, and 130 healthy individuals by AlphaLISA. There was a significant difference between RCC patients (405 $\pm$ 153 μg/ml) and healthy individuals (294 $\pm$ 102 μg/ml) with a p-value of 1.8×10^{-7} (Mann-Whitney U test) (Fig. 2a). The plasma concentration of FN1 was not elevated in PCa patients (306 $\pm$ 81 μg/ml). The AUC value of ROC for plasma FN1 concentration of RCC patients to healthy individuals was calculated to be 0.71 for all stages, stage I and II and stage III and IV (Fig. 2b). *The optimum diagnostic cut-off point of FN1 was identified at 377 μg/ml by the AUC curve. At this point, sensitivity, specificity, PPV and NPV were 53%, 82%, 64% and 75% respectively. And the fibronectin concentration in each clinical stage was shown in Fig. 2c.*

3.4. *Correlation of plasma concentration of FN1 and clinicopathological parameters*

The statistical analyses were performed to *detect* the correlation of plasma concentration of FN1 and clinical stage (Fig. 2c), but there were no significant differences. Also, there were no significant correlations between concentration of FN1 and the other clinicopathological parameters, such as tumor size, tumor grade and vascular involvement (data not shown). Furthermore, Kaplan–Meier analysis, used to analyze the correlation

Table 2
Summary of protein identification by tandem mass spectrometry

ID	m/z	RT	Charge	Control (mean ± SD)	RCC (mean ± SD)	P Values**	Mascot Score	Peptide sequence	Protein description
2411	799.3815	36.479	3	15±6	25±13	5.09E-03	84.46	RPGGEPSPEGTTGQSYNQYSQR	Fibronectin
3454	622.3328	39.679	3	14±4	20±8	8.59E-03	75.78	HTSVQTTSSGSGPFTDVR	Fibronectin
3948	647.3662	49.283	2	13±2	17±7	9.54E-03	54.92	DLQFVEVTDVK	Fibronectin
2039	978.5337	47.716	2	16±7	30±20	6.08E-03	53.45	EESPLLIGQQSTVSDVPR	Fibronectin
750	706.3586	44.432	2	101±45	73±28	2.34E-02	51.41	KWQEEMELYR	Apolipoprotein A-I
2614	815.4614	46.26	2	11±4	18±12	1.61E-02	50.73	VDVIPVNLPGEHGQR	Fibronectin
2068	646.379	52.817	2	17±7	26±15	1.96E-02	46.43	GATYNIIVEALK	Fibronectin
2854	997.5346	53.967	2	18±5	23±11	4.61E-02	41.28	NTFAEVTGLSPGVTYYFK	Fibronectin
1231	675.3681	45.847	2	28±11	52±34	4.38E-03	40.93	WLPSSSPVTGYR	Fibronectin
1816	772.8941	45.207	2	17±7	32±20	5.88E-03	35.57	SYTITGLQPGTDYK	Fibronectin
2439	638.3344	38.15	2	22±7	30±13	1.54E-02	32.64	HVVPNEVVVQR	Gelsolin
2569	555.8103	40.153	2	16±5	25±13	6.00E-03	32.26	STTPDITGYR	Fibronectin
1155	772.419	45.123	2	43±14	64±34	1.27E-02	31.79	SYTITGLQPGTDYK	Fibronectin
2771	701.8697	39.773	2	13±5	22±13	6.58E-03	30.7	HYQINQQWER	Fibronectin
2611	592.8548	43.895	2	26±11	19±6	1.87E-02	30.31	IQNILTEEPK	Serum paraoxonase
1371	511.785	35.131	2	44±12	55±17	1.82E-02	29.99	ATVVYQGER	Beta-2-glycoprotein 1
1826	867.5129	50.364	2	20±7	36±22	3.48E-03	29.17	NLQPASEYTVSLVAIK	Fibronectin
1813	701.366	39.859	2	28±7	42±18	4.02E-03	27.25	HYQINQQWER	Fibronectin
2417	576.8117	42.453	2	16±5	26±15	5.75E-03	26.67	FTNIGPDTMR	Fibronectin
1794	964.0527	58.428	2	23±8	34±20	2.61E-02	23.59	VTWAPPPSIDLTNFLVR	Fibronectin
1377	629.36	53.672	2	39±23	24±9	7.97E-03	21.25	DLAVVDAKDAIK	EXOC1_HUMAN

RT, retention time; RCC, renal cell carcinoma
**Welch's t-test.

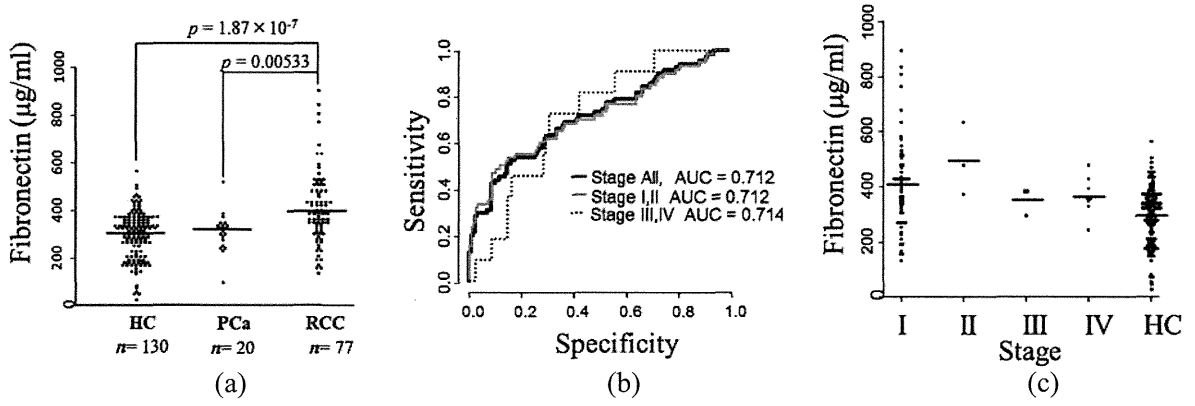

Fig. 2. (a) Concentration of plasma FN1 in each group. The FN1 concentration of renal cell carcinoma patients ($n = 77$), healthy individuals ($n = 130$) and prostate cancer patients ($n = 20$) was measured by AlphaLISA. There were significant differences in renal cell carcinoma patients compared to healthy individuals and prostate cancer patients, but not between healthy individuals and prostate cancer patients (Mann-Whitney U test). Horizontal lines represent the average concentration. (b) Receiver operating characteristic (ROC) curve for plasma FN1 concentration. AUC value of ROC for plasma FN1 concentration of RCC patients to healthy individuals was calculated to be 0.71 for all stages, stage I and II and stage III and IV. Similar AUC value of earlier stage to advanced stage suggested the possibility of early detection of renal cell carcinoma by plasma FN1. (c) The plasma FN1 concentration in each clinical stage. HC; healthy control.

of serum value of FN1, cancer-specific survival and overall survival, failed to prove any statistical significant differences with a median follow up of 47.6 months after surgery (data not shown).

4. Discussion

FN1 is a high-molecular-weight extracellular matrix protein that plays an important role in cellular attachment and cell spread [14,15]. FN1 can be soluble or insoluble, is produced by hepatocytes and various cell types and is bound to integrins [16]. Altered expression of FN1 is known to change the morphology of several tumor cell lines [17]. In several studies of different RCC cell lines, FN1 was shown to be secreted into the culture medium and suggested to influence the movement and invasion of these cells [18–20]. Another study showed FN1 plasma levels signif-

icantly elevated in localized and metastatic RCC patients compared to a control group [21]. According to "THE HUMAN PROTEIN ATLAS" (http://www. proteinatlas.org/ENSG00000115414), FN1 is expressed *in* extracellular matrix and stromal cell. FN1 is expressed weakly in normal kidney and relatively higher expressed in kidney cancer. It could be considerable that higher plasma levels of FN1 is secreted from these extracellular matrix and stromal cell in kidney cancer. A recent study suggested that FN1 mRNA expression was higher in RCC compared to normal renal tissue and correlated with advanced disease, suggesting that FN1 mRNA expression might serve as a marker for RCC aggressiveness [22]. Although the researchers failed to measure the plasma concentration of FN1, this study supports the results described herein obtained by proteome based screening.

The results of plasma FN1 from 2DICAL analysis were validated in a hundreds-scale cohort using a different methodology. AlphaLISA confirmed that the plasma level of FN1 was up-regulated in the early stage of RCC, which suggested that the FN1 plasma levels might be a tool for screening and diagnosis of RCC. However, there a limitation to introduce FN1 for screening of RCC, because plasma concentrations between patients and controls were overlapped extensively, and FN1 was not examined in benign renal tumors.

RCC comprises five histologically distinct subtypes classified by morphologic and pathologic features including clear cell (75%), papillary (10–15%), chromophobe (5–10%), collecting duct, and unclassified subtypes. We have previously reported that each RCC subtype has a totally different genetic profile by whole genome SNP array [10]. Therefore, each subtype should have a specific biomarker. In this study, we focused on clear cell RCC because it is the most abundant subtype of RCC and hence should be a first target of screening. Our comprehensive study of proteomics led to the possibility that monitoring the level of plasma FN1 could be clinically useful for the screening and diagnosis of RCC patients. The most of the *patients* we analyze were clinical stage I (56 cases / total 77 cases), and they had no symptoms such as febrile and *showed* normal range of C-reactive protein. Therefore, we believe that FN1 was not derived from acute phase reaction. Reports of the elevation of the plasma level of FN1 in RCC exist in the literature [21], but its clinical usage has not yet been described. One of the reasons may be the lack of applicable clinical test such as ELISA for FN1. The assessment of plasma FN1 levels must be determined for a large scale clinical cohort, but the construction of an easy clinical test such as ELISA will be needed for its completion.

Acknowledgments

We thank Ms. Ayako Igarashi, Ms. Tomoko Umaki, and Ms. Yuka Nakamura for their technical assistance.

Disclosure of potential conflicts of interest

These sponsors had no role in the design of the study, the collection of the data, the analysis and interpretation of the data, the decision to submit the manuscript for publication, or the writing of the manuscript.

Grant supports

Funding was received from the Program for Promotion of Fundamental Studies in Health Sciences conducted by the National Institute of Biomedical Innovation of Japan, and the Third-Term Comprehensive Control Research for Cancer and Research on Biological Markers for New Drug Development conducted by the Ministry of Health, Labour and Welfare of Japan.

Conflicts of interest

None.

References

[1] S.H. Landis, T. Murray, S. Bolden, P.A. Wingo. Cancer statistics, 1999, CA Cancer J Clin 49 (1999), 8-31.
[2] A.J. Schrader, Z. Varga, A. Hegele, S. Pfoertner, P. Olbert, R. Hofmann. Second-line strategies for metastatic renal cell carcinoma: classics and novel approaches, J Cancer Res Clin Oncol 132 (2006), 137-149.
[3] B.I. Rini, S. Halabi, R. Barrier, K.A. Margolin, D. Avigan, T. Logan et al. Adoptive immunotherapy by allogeneic stem cell transplantation for metastatic renal cell carcinoma: a CALGB intergroup phase II study, Biol Blood Marrow Transplant 12 (2006), 778-785.
[4] C. Gouttefangeas, A. Stenzl, S. Stevanovic, H.G. Rammensee. Immunotherapy of renal cell carcinoma, Cancer Immunol Immunother 56 (2007), 117-128.
[5] M. Remzi, M. Marberger. Renal tumor biopsies for evaluation of small renal tumors: why, in whom, and how? Eur Urol 55 (2009), 359-367.
[6] M. Ono, M. Shitashige, K. Honda, T. Isobe, H. Kuwabara, H. Matsuzuki et al. Label-free quantitative proteomics using large peptide data sets generated by nanoflow liquid chromatography and mass spectrometry, Mol Cell Proteomics 5 (2006), 1338-1347.

[7] M. Ono, J. Matsubara, K. Honda, T. Sakuma, T. Hashiguchi, H. Nose et al. Prolyl 4-hydroxylation of alpha-fibrinogen: a novel protein modification revealed by plasma proteomics, J Biol Chem 284 (2009), 29041-29049.
[8] A. Negishi, M. Ono, Y. Handa, H. Kato, K. Yamashita, K. Honda et al. Large-scale quantitative clinical proteomics by label-free liquid chromatography and mass spectrometry, Cancer Sci 100 (2009), 514-519.
[9] J. Matsubara, M. Ono, A. Negishi, H. Ueno, T. Okusaka, J. Furuse et al. Identification of a predictive biomarker for hematologic toxicities of gemcitabine, J Clin Oncol 27 (2009), 2261-2268.
[10] A. Yokomizo, K. Yamamoto, K. Furuno, M. Shiota, K. Tatsugemi, K. Kuroiwa et al. Histopathologic subtype-specific genomic profiles of renal cell carcinomas identified by high-resolution whole-genome single nucleotide polymorphism array analysis, Oncol Lett 1 (2010), 1073-1078.
[11] TNM Classification of Malignant Tumours. John Wiley and Sons Ltd 2009.
[12] M. Shitashige, R. Satow, K. Honda, M. Ono, S. Hirohashi, T. Yamada. Regulation of Wnt signaling by the nuclear pore complex, Gastroenterology 134 (2008), 1961-1971, 1971 e1961-1964.
[13] J.D. Storey, R. Tibshirani. Statistical significance for genome-wide studies, Proc Natl Acad Sci USA 100 (2003), 9440-9445.
[14] S.M. Albelda. Role of integrins and other cell adhesion molecules in tumor progression and metastasis, Lab Invest 68 (1993), 4-17.
[15] R.O. Hynes, K.M. Yamada. Fibronectins: multifunctional modular glycoproteins, J Cell Biol 95 (1982), 369-377.
[16] R. Pankov, K.M. Yamada. Fibronectin at a glance, J Cell Sci 115 (2002), 3861-3863.
[17] H. Ro. Fibronectins. Berlin, Heidelberg, New York: Springer.
[18] W. Brenner, S. Gross, F. Steinbach, S. Horn, R. Hohenfellner, J.W. Thuroff. Differential inhibition of renal cancer cell invasion mediated by fibronectin, collagen IV and laminin, Cancer Lett 155 (2000), 199-205.
[19] J. Lohi, T. Tani, I. Leivo, A. Linnala, L. Kangas, R.E. Burgeson et al. Expression of laminin in renal-cell carcinomas, renal-cell carcinoma cell lines and xenografts in nude mice, Int J Cancer 68 (1996), 364-371.
[20] J. Murata, I. Saiki, J. Yoneda, I. Azuma. Differences in chemotaxis to fibronectin in weakly and highly metastatic tumor cells, Jpn J Cancer Res 83 (1992), 1327-1333.
[21] A. Hegele, A. Heidenreich, J. Kropf, R. von Knobloch, Z. Varga, R. Hofmann et al. Plasma levels of cellular fibronectin in patients with localized and metastatic renal cell carcinoma, Tumour Biol 25 (2004), 111-116.
[22] S. Waalkes, F. Atschekzei, M.W. Kramer, J. Hennenlotter, G. Vetter, J.U. Becker et al. Fibronectin 1 mRNA expression correlates with advanced disease in renal cancer, BMC Cancer 10 (2010), 503.

Supplemental material

MS/MS Fragmentation of **RPGGEPSPEGTTGQSYNQYSQR**
Found in **FINC_HUMAN**, Fibronectin OS=Homo sapiens GN=FN1 PE=1 SV=3
Match to Query 1: 2395.118583 from(799.380137,3+)

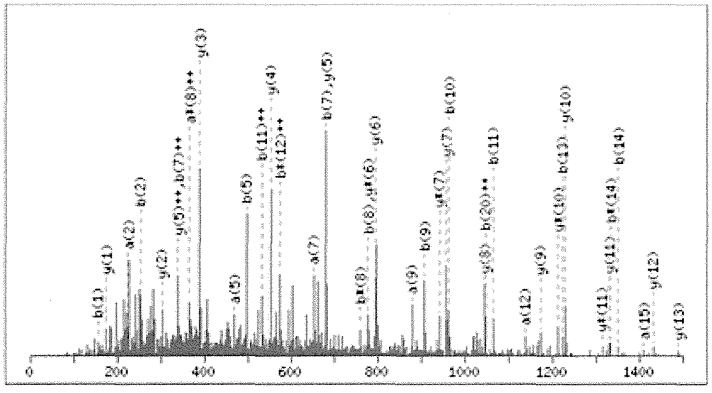

Monoisotopic mass of neutral peptide Mr(calc): 2395.0789
Ions Score: 84 **Expect:** 6.3e-008
Matches (Bold Red): 41/252 fragment ions using 78 most intense peaks

#	a	a^{++}	a*	a*$^{++}$	b	b^{++}	b*	b*$^{++}$	Seq.	y	y^{++}	y*	y*$^{++}$	#
1	129.1135	65.0604	112.0869	56.5471	157.1084	79.0578	140.0818	70.5446	R					22
2	226.1662	113.5868	209.1397	105.0735	254.1612	127.5842	237.1346	119.0709	P	2239.985	1120.4962	2222.9585	1111.9829	21
3	283.1877	142.0975	266.1612	133.5842	311.1826	156.0949	294.1561	147.5817	G	2142.9323	1071.9698	2125.9057	1063.4565	20
4	340.2092	170.6082	323.1826	162.0949	368.2041	184.6057	351.1775	176.0924	G	2085.9108	1043.459	2068.8843	1034.9458	19
5	469.2518	235.1295	452.2252	226.6162	497.2467	249.127	480.2201	240.6137	E	2028.8894	1014.9483	2011.8628	1006.435	18
6	566.3045	283.6559	549.278	275.1426	594.2994	297.6534	577.2729	289.1401	P	1899.8468	950.427	1882.8202	941.9137	17
7	653.3365	327.1719	636.31	318.6586	681.3315	341.1694	664.3049	332.6561	S	1802.794	901.9006	1785.7674	893.3874	16
8	750.3893	375.6983	733.3628	367.185	778.3842	389.6958	761.3577	381.1825	P	1715.762	858.3846	1698.7354	849.8713	15
9	879.4319	440.2196	862.4054	431.7063	907.4268	454.217	890.4003	445.7038	E	1618.7092	809.8582	1601.6827	801.345	14
10	936.4534	468.7303	919.4268	460.217	964.4483	482.7278	947.4217	474.2145	G	1489.6666	745.3369	1472.6401	736.8237	13
11	1037.501	519.2542	1020.4745	510.7409	1065.496	533.2516	1048.4694	524.7383	T	1432.6451	716.8262	1415.6186	708.3129	12
12	1138.5487	569.778	1121.5222	561.2647	1166.5436	583.7755	1149.5171	575.2622	T	1331.5975	666.3024	1314.5709	657.7891	11
13	1195.5702	598.2887	1178.5436	589.7755	1223.5651	612.2862	1206.5386	603.7729	G	1230.5498	615.7785	1213.5232	607.2653	10
14	1323.6288	662.318	1306.6022	653.8047	1351.6237	676.3155	1334.5971	667.8022	Q	1173.5283	587.2678	1156.5018	578.7545	9
15	1410.6608	705.834	1393.6342	697.3208	1438.6557	719.8315	1421.6292	711.3182	S	1045.4697	523.2385	1028.4432	514.7252	8
16	1573.7241	787.3657	1556.6976	778.8524	1601.719	801.3632	1584.6925	792.8499	Y	958.4377	479.7225	941.4112	471.2092	7
17	1687.7671	844.3872	1670.7405	835.8739	1715.762	858.3846	1698.7354	849.8713	N	795.3744	398.1908	778.3478	389.6776	6
18	1815.8256	908.4165	1798.7991	899.9032	1843.8205	922.4139	1826.794	913.9006	Q	681.3315	341.1694	664.3049	332.6561	5

Fig. S1. Mascot report of one representative fragment of FN1.

```
1     MLRGPGPGLL LLAVQCLGTA VPSTGASKSK RQAQQMVQPQ SPVAVSQSKP
51    GCYDNGKHYQ INQQWERTYL GNALVCTCYG GSRGFNCESK PEAEETCFDK
101   YTGNTYRVGD TYERPKDSMI WDCTCIGAGR GRISCTIANR CHEGGQSYKI
151   GDTWRRPHET GGYMLECVCL GNGKGEWTCK PIAEKCFDHA AGTSYVVGET
201   WEKPYQGWMM VDCTCLGEGS GRITCTSRNR CNDQDTRTSY RIGDTWSKKD
251   NRGNLLQCIC TGNGRGEWKC ERHTSVQTTS SGSGPFTDVR AAVYQPQPHP
301   QPPPYGHCVT DSGVVYSVGM QWLKTQGNKQ MLCTCLGNGV SCQETAVTQT
351   YGGNSNGEPC VLPFTYNGRT FYSCTTEGRQ DGHLWCSTTS NYEQDQKYSF
401   CTDHTVLVQT QGGNSNGALC HFPFLYNNHN YTDCTSEGRR DNMKWCGTTQ
451   NYDADQKFGF CPMAAHEEIC TTNEGVMYRI GDQWDKQHDM GHMMRCTCVG
501   NGRGEWTCIA YSQLRDQCIV DDITYNVNDT FHKRHEEGHM LNCTCFGQGR
551   GRWKCDPVDQ CQDSETGTFY QIGDSWEKYV HGVRYQCYCY GRGIGEWHCQ
601   PLQTYPSSSG PVEVFITETP SQPNSHPIQW NAPQPSHISK YILRWRPKNS
651   VGRWKEATIP GHLNSYTIKG LKPGVVYEGQ LISIQQYGHQ EVTRFDFTTT
701   STSTPVTSNT VTGETTPFSP LVATSESVTE ITASSFVVSW VSASDTVSGF
751   RVEYELSEEG DEPQYLDLPS TATSVNIPDL LPGRKYIVNV YQISEDGEQS
801   LILSTSQTTA PDAPPDPTVD QVDDTSIVVR WSRPQAPITG YRIVYSPSVE
851   GSSTELNLPE TANSVTLSDL QPGVQYNITI YAVEENQEST PVVIQQETTG
901   TPRSDTVPSP RDLQFVEVTD VKVTIMWTPP ESAVTGYRVD VIPVNLPGEH
951   GQRLPISRNT FAEVTGLSPG VTYYFKVFAV SHGRESKPLT AQQTTKLDAP
1001  TNLQFVNETD STVLVRWTPP RAQITGYRLT VGLTRRGQPR QYNVGPSVSK
1051  YPLRNLQPAS EYTVSLVAIK GNQESPKATG VFTTLQPGSS IPPYNTEVTE
1101  TTIVITWTPA PRIGFKLGVR PSQGGEAPRE VTSDSGSIVV SGLTPGVEYV
1151  YTIQVLRDGQ ERDAPIVNKV VTPLSPPTNL HLEANPDTGV LTVSWERSTT
1201  PDITGYRITT TPTNGQQGNS LEEVVHADQS SCTFDNLSPG LEYNVSVYTV
1251  KDDKESVPIS DTIIPAVPPP TDLRFTNIGP DTMRVTWAPP PSIDLTNFLV
1301  RYSPVKNEED VAELSISPSD NAVVLTNLLP GTEYVVSVSS VYEQHESTPL
1351  RGRQKTGLDS PTGIDFSDIT ANSFTVHWIA PRATITGYRI RHHPEHFSGR
1401  PREDRVPHSR NSITLTNLTP GTEYVVSIVA LNGREESPLL IGQQSTVSDV
1451  PRDLEVVAAT PTSLLISWDA PAVTVRYYRI TYGETGGNSP VQEFTVPGSK
1501  STATISGLKP GVDYTITVYA VTGRGDSPAS SKPISINYRT EIDKPSQMQV
1551  TDVQDNSISV KWLPSSSPVT GYRVTTTPKN GPGPTKTKTA GPDQTEMTIE
1601  GLQPTVEYVV SVYAQNPSGE SQPLVQTAVT NIDRPKGLAF TDVDVDSIKI
1651  AWESPQGQVS RYRVTYSSPE DGIHELFPAP DGEEDTAELQ GLRPGSEYTV
1701  SVVALHDDME SQPLIGTQST AIPAPTDLKF TQVTPTSLSA QWTPPNVQLT
1751  GYRVRVTPKE KTGPMKEINL APDSSSVVVS GLMVATKYEV SVYALKDTLT
1801  SRPAQGVVTT LENVSPPRRA RVTDATETTI TISWRTKTET ITGFQVDAVP
1851  ANGQTPIQRT IKPDVRSYTI TGLQPGTDYK IYLYTLNDNA RSSPVVIDAS
1901  TAIDAPSNLR FLATTPNSLL VSWQPPRARI TGYIIKYEKP GSPPREVVPR
1951  PRPGVTEATI TGLEPGTEYT IYVIALKNNQ KSEPLIGRKK TDELPQLVTL
2001  PHPNLHGPEI LDVPSTVQKT PFVTHPGYDT GNGIQLPGTS GQQPSVGQQM
2051  IFEEHGFRRT TPPTTATPIR HRPRPYPPNV GEEIQIGHIP REDVDYHLYP
2101  HGPGLNPNAS TGQEALSQTT ISWAPFQDTS EYIISCHPVG TDEEPLQFRV
2151  PGTSTSATLT GLTRGATYNI IVEALKDQQR HKVREEVVTV GNSVNEGLNQ
2201  PTDDSCFDPY TVSHYAVGDE WERMSESGFK LLCQCLGFGS GHFRCDSSRW
2251  CHDNGVNYKI GEKWDRQGEN GQMMSCTCLG NGKGEFKCDP HEATCYDDGK
2301  TYHVGEQWQK EYLGAICSCT CFGGQRGWRC DNCRRPGGEP SPEGTTGQSY
2351  NQYSQRYHQR TNTNVNCPIE CFMPLDVQAD REDSRE
```

Matched peptides shown in **Bold Red**

Fig. S2. Peptide hits in the FN1 sequence indicated in red.

International Scholarly Research Network
ISRN Oncology
Volume 2012, Article ID 768190, 10 pages
doi:10.5402/2012/768190

Clinical Study

Carbonic Anhydrase I as a New Plasma Biomarker for Prostate Cancer

Michiko Takakura,[1] Akira Yokomizo,[2] Yoshinori Tanaka,[3] Michimoto Kobayashi,[3] Giman Jung,[3] Miho Banno,[4] Tomohiro Sakuma,[4] Kenjiro Imada,[2,5] Yoshinao Oda,[5] Masahiro Kamita,[1] Kazufumi Honda,[1] Tesshi Yamada,[1] Seiji Naito,[2] and Masaya Ono[1]

[1] *Division of Chemotherapy and Clinical Research, National Cancer Center Research Institute, 5-1-1 Tsukiji, Chuo-ku, Tokyo 104-0045, Japan*
[2] *Department of Urology, Graduate School of Medical Sciences, Kyushu University, 3-1-1 Maidashi, Higashi-ku, Fukuoka 812-8582, Japan*
[3] *New Frontiers Research Laboratories, Toray Industries, Inc., 10-1 Tebiro, Kanagawa, Kamakura 248-8555, Japan*
[4] *Bio Science Department, Research and Development Center, Mitsui Knowledge Industry Co., Ltd., 2-7-14 Higashinakano, Nakano-Ku, Tokyo 164-8555, Japan*
[5] *Department of Anatomic Pathology, Graduate School of Medical Sciences, Kyushu University, 3-1-1 Maidashi, Higashi-ku, Fukuoka 812-8582, Japan*

Correspondence should be addressed to Masaya Ono, masono@ncc.go.jp

Received 17 September 2012; Accepted 2 October 2012

Academic Editors: A. E. Bilsland, B. Comin-Anduix, G. Ferrandina, and S. Holdenrieder

Serum prostate-specific antigen (PSA) levels ranging from 4 to 10 ng/mL is considered a diagnostic gray zone for detecting prostate cancer because biopsies reveal no evidence of cancer in 75% of these subjects. Our goal was to discover a new highly specific biomarker for prostate cancer by analyzing plasma proteins using a proteomic technique. Enriched plasma proteins from 25 prostate cancer patients and 15 healthy controls were analyzed using a label-free quantitative shotgun proteomics platform called 2DICAL (2-dimensional image converted analysis of liquid chromatography and mass spectrometry) and candidate biomarkers were searched. Among the 40,678 identified mass spectrum (MS) peaks, 117 peaks significantly differed between prostate cancer patients and healthy controls. Ten peaks matched carbonic anhydrase I (CAI) by tandem MS. Independent immunological assays revealed that plasma CAI levels in 54 prostate cancer patients were significantly higher than those in 60 healthy controls ($P = 0.022$, Mann-Whitney U test). In the PSA gray-zone group, the discrimination rate of prostate cancer patients increased by considering plasma CAI levels. CAI can potentially serve as a valuable plasma biomarker and the combination of PSA and CAI may have great advantages for diagnosing prostate cancer in patients with gray-zone PSA level.

1. Introduction

Prostate cancer is the most common malignancy in the United State. In 2009, 192,280 men were estimated to have been diagnosed with prostate cancer, and 27,360 of these patients died in the United States [1]. The prostate-specific antigen (PSA) is used for the detection of prostate cancer in daily practice, but its diagnostic reliability is hampered by its low specificity. Thus, serum PSA levels ranging from 4 to 10 ng/mL are called the "gray zone" in which it is very difficult to discriminate between patients with prostate cancer and those with benign prostatic hyperplasia (BPH), prostatitis, or normal prostate. Furthermore, among the patients with serum PSA levels between 4 to 10 ng/mL, only 25% will be found to have prostate cancer [2]. Serum PSA levels can also increase in prostatitis, [3, 4] and approximately 20%–30% of prostate cancers are missed when the cut-off value is set to 4 ng/mL [5–7]. The false negative rate in the first biopsy is estimated between 12% and 32% [8, 9], and a large population of men with chronically high serum PSA

levels undergo repeated biopsies to eliminate the possibility of prostate cancer [3, 4].

Our quantitative label-free shotgun proteomics analysis system, called 2-dimensional image converted analysis of liquid chromatography and mass spectrometry (2DICAL), can accurately align different liquid chromatography-mass spectrometry (LC-MS) data sets, enabling rapid comparison of a statistically sufficient number of clinical samples [10–16]. 2DICAL has a characteristic of top-down proteomics in shotgun proteomics. It converts the LC-MS spectrum data into peaks on a 2-dimensional plane with axes of mass-to-charge ratio (m/z) and retention time (RT). The peaks with the same m/z and RT are compared across the samples, and statistically significant peaks are selected. Targeted tandem mass spectrometry (MS) is conducted on the selected peaks, and the peaks are annotated by sequence search programs (see Supplemental Materials available online at doi: 10.5402/2012/768190).

Here we describe the discovery of a new candidate biomarker for prostate cancer diagnosis that we uncovered using 2DICAL to compare the plasma proteomes of prostate cancer patients with those of healthy controls.

2. Materials and Methods

2.1. Clinical Samples. Plasma samples were prospectively collected at the Department of Urology and Ophthalmology, Graduate School of Medical Sciences, Kyushu University (Fukuoka, Japan), between October 2000 and January 2008 from 162 individuals, including those suffering from prostate cancer ($n = 54$), renal cell cancer (RCC; $n = 20$), prostatitis ($n = 6$), and BPH ($n = 22$) and 60 healthy individuals who had no symptom and PSA below 10 ng/mL, and those with PSA over 4 ng/mL were periodically followed in outpatient clinic with no evidence of prostate cancer. Prostate cancer patients were definitively diagnosed by prostate biopsy. Patient characteristics including age, PSA levels, Gleason score, and TNM classification are shown in Table 1. For 2DICAL analysis, we selected prostate cancer patients and age-matched healthy controls. All patients provided written informed consent authorizing the collection and use of their samples for research. The institutional ethics committee boards of the National Cancer Center Research Institute (Tokyo, Japan) and the Kyushu University reviewed and approved our protocol.

2.2. Sample Preparation. To exclude sampling bias, 7 mL of each patient's whole blood was collected in a tube containing ethylenediaminetetraacetic acid-2Na (Venoject II, Terumo, Japan) before surgery or first treatment. Plasma was prepared by centrifuging samples at 1,050 ×g for 10 min at 4°C. Aliquots of 1 mL were added to 1.5-mL Eppendorf tubes and frozen at −80°C until analysis. Control samples were collected and stored identically. All samples were subjected to only 1 freeze-thaw cycle. To enrich low molecular weight plasma proteins, 500 μL of plasma was diluted to 4 mL by adding 25 mM ammonium bicarbonate buffer (pH 8.0), and the diluted plasma samples were processed using a hollow fiber membrane-based low molecular weight (LMW) protein enrichment device as described previously [14, 17]. The device employs multistage filtration and cascaded cross-flow processes, and the proteins smaller than a predetermined molecular weight can be separated in a fully automated operation. The solution enriched for LMW proteins was recovered for 1 h operation and the LMW proteins were digested at 37°C for 18 h with sequencing grade modified trypsin (Promega, Madison, WI).

2.3. LC-MS. Trypsin-digested samples were analyzed in duplicate by nanoflow high-performance liquid chromatography (NanoFrontier nLC, Hitachi High-technologies, Tokyo, Japan) connected to an electrospray ionization quadrupole time-of-flight mass spectrometer (Q-Tof Ultima, Waters, Milford, MA). MS peaks were detected, normalized, and quantified using our 2DICAL software package [10, 12]. A serial identification (ID) number was applied to each of the MS peaks detected. The reproduction of LC-MS was monitored by calculating the correlation coefficient (CC) and coefficient of variance (CV) of every measurement.

2.4. Protein Identification by Tandem Mass Spectrometry (MS/MS). Peak lists were generated using the Mass Navigator software package (Mitsui Knowledge Industry, Tokyo, Japan) and searched against the SwissProt database using the Mascot software package (Matrix Science, London, UK). Search parameters used were as follows: human protein sequences were selected, trypsin was designated as the enzyme, and up to 1 missed cleavage was allowed. Mass tolerances for precursor and fragment ions were ±0.6 Da and ±0.2 Da, respectively. The score threshold was set to a Mascot score >30. If a peptide matched to multiple proteins, the protein name with the highest Mascot score was selected.

2.5. Western Blot Analysis. Plasma samples were analyzed by sodium dodecyl sulfate-polyacrylamide gel electrophoresis using 10%–20% (w/v) ready-made gels (Pagel; ATTO, Tokyo, Japan) with the Laemmli buffer and electroblotted to a polyvinylidene difluoride membrane (Millipore, Billerica, MA). Primary antibodies were goat polyclonal carbonic anhydrase I (CAI) antibody (Millipore, Billerica, MA) and mouse monoclonal antibody against human complement C3b-α (PROGEN, Heidelberg, Germany). The membrane was incubated with the primary antibodies and then with the relevant horseradish peroxidase (HRP)-conjugated anti-goat or anti-mouse IgG as described previously [18]. Blots were developed using an enhanced chemiluminescence plus detection system (GE Healthcare, Buckinghamshire, UK).

2.6. Enzyme-Linked Immunosorbent Assay (ELISA). To develop sandwich ELISA, the capture antibody (rabbit polyclonal CAI antibody, Abnova, Taipei, Taiwan) was immobilized on a 96-well plate (Thermo Fisher Scientific, MA) at a final concentration of 2.5 μg/mL and incubated at 4°C overnight. A mouse monoclonal CAI antibody (0.5 μg/mL; Abnova, Taipei, Taiwan) was used as the detection antibody. After incubation with HRP-conjugated goat anti-mouse IgG (Vector Laboratories, Burlingame, CA) for 1 h and then with